Model-potential approach to metal surfaces

P. Raghavendra Rao and G. Mukhopadhyay
Physics Department, Indian Institute of Technology, Powai, Bombay 400076, India
(Received 29 June 1984)

A simple and realistic model potential of Woods-Saxon type is used to determine the one-electron states for a semi-infinite metal (jellium). The various potential parameters are determined by the use of certain physical constraints which ensure the self-consistency approximately. To judge the accuracy and the effectiveness of this potential model, we compare the work-function values obtained in the present scheme with those of the fully self-consistent calculations of Lang and Kohn. We also extend the present analysis incorporating the lattice effects via local-pseudopotential theory to obtain the work-function values for a few simple real metals, and the results are compared with the polycrystalline experimental values.

I. INTRODUCTION

A detailed study of metal surfaces is needed in view of the latest developments in experimental techniques (both elastic and inelastic low-energy electron diffraction experiments, molecular beam scattering, etc.). Many of the various metal surface properties and their related phenomena (e.g., photoemission, response to external field, etc.) can be understood via the ground-state one-electron wave functions (OEWF). Normally these OEWF are obtained through the self-consistent local-field approximation of Lang and Kohn[1] (LK) [local-density approximation (LDA)] using the Kohn-Sham approach of density-functional theory[2] (DFT). In this approach a set of Schrödinger-type equations for particles moving in an effective potential are solved numerically. The effective potential is written as a sum of electrostatic potential and a local exchange and correlation potential which are functionals of electronic charge density that must then be determined self-consistently from OEWF. This procedure is rather involved numerically, so that even for a simple metal with planar surface represented by a semi-infinite jellium, heavy computation is essential making its utilization (e.g., photoemission[3]) completely numerically oriented at the outset. To circumvent this problem, attempts have been made to use simple models for the one-electron effective potential for a semi-infinite jellium. Such model potentials do give fairly accurate results for ground-state properties compared with other LDA calculations.[4,5] With this in mind, we present here a parametrized one-electron potential, $V(x)$ of Woods-Saxon type, to obtain OEWF in analytic form.[6] The parameters will be determined iteratively with the imposition of certain physical conditions. These physical constraints will ensure, though approximately, the self-consistency of the potential. The constraints used here follow from the intrinsic requirement of total charge neutrality, the self-consistency in the surface dipole barrier, and the application of a theorem due to Budd and Vannimenus[7] (BVT). The last requirement has been used before by Sahni *et al.*[5] for the finite-linear-potential-model calculations, producing the work-function and surface-energy values of reasonable accuracy.

We use a semi-infinite jellium model to represent the metal wherein the positive background is extended over the region $x>0$ with yz plane parallel to the planar surface. The model potential considered here is of the form (see Fig. 1)

$$V(x)=\frac{V_0}{1+\exp[(x-x_0)/a]}\ , \tag{1}$$

where the parameters V_0, x_0, and a are to be found. This model potential has the advantages over the earlier proposed finite-Barrier[4] (FB) potential and finite-linear[5] (FL) potential models in that it has continuous derivatives with respect to x, and does not require finding the solutions in different regions of x and then matching them and their first derivatives at the interface of these regions. This also has a feature that as $a\to 0$, this potential model reduces to a finite-step-barrier model. Below we obtain for this potential the OEWF in terms of hypergeometric series, which may be used for further studies, viz., linear response functions, etc. These solutions are mathematically and computationally simple and many of the spatial integrals related to parameter-determining constraints can be performed analytically. We present here the calculations of work-function (Φ^J) values for jellium model and

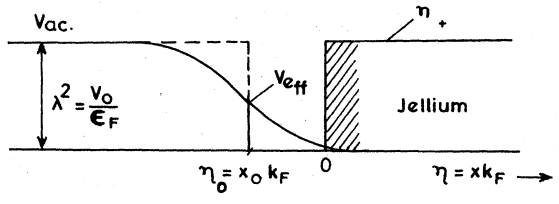

FIG. 1. Schematic representation of the jellium model and the one-electron effective potential v_{eff} of Woods-Saxon type.

compare them with the fully self-consistent LDA results, in order to judge the effectiveness and the accuracy of the present model. A preliminary account of this has already been communicated.[8] We also present the work-function (Φ) values for a few simple metals incorporating the ion-lattice effects through the local-pseudopotential theory, following Sahni and Gruenebaum.[9] They treat the contribution of the difference $\delta v(\vec{r})$ between the pseudopotentials of the semi-infinite lattice of ions and the electrostatic potential of the jellium background as an additional term in the total energy functional, thereafter treating the total energy variationally. This is different from the approach of LK who have introduced these ion-lattice effects via first-order perturbation theory. In Sec. II we present a detailed analysis to obtain the expressions for density profile, dipole barrier, electrostatic potential, and metal surface position parameter. We also specify the physical constraints and obtain expressions for them in terms of the three potential parameters, namely, V_0, x_0, and a. In Sec. III we present the results and conclusions.

II. THEORY

The OEWF for the semi-infinite system are written as

$$\Psi(x,y,z)=\psi(x)\frac{e^{ik_y y+ik_z z}}{2\pi}\ , \tag{2}$$

where $\psi(x)$ satisfies the equation (in atomic units, where $\hbar=1=e^2=m_e$)

$$\left[-\frac{1}{2}\frac{d^2}{dx^2}+V(x)-E\right]\psi(x)=-\frac{k^2}{2}\psi(x)\ , \tag{3}$$

with $V(x)$ given by Eq. (1). Here $k^2=k_z^2+k_y^2$ and E is the energy of the state. For convenience, we introduce dimensionless variables as $\eta=xk_F$, $\eta_0=x_0k_F$, and $E-\frac{1}{2}k^2=t^2\epsilon_F$, where k_F is the Fermi wave vector and ϵ_F is the Fermi energy of the metal. In terms of these new variables, the potential has the form

$$v(\eta)=\frac{V(\eta)}{\epsilon_F}=\frac{\lambda^2}{1+\exp[(\eta-\eta_0)/\alpha]}\ , \tag{4}$$

where $V_0=\lambda^2\epsilon_F$ and $\alpha=ak_F$. The wave equation [Eq. (3)] now takes the form

$$\left[\frac{d^2}{d\eta^2}-v(\eta)+t^2\right]\psi_t(\eta)=0\ . \tag{5}$$

The electron charge density is obtained as $\rho(\eta)=n_-(\eta)\rho(\eta\to\infty)$ where $n_-(\eta)$ is the electron density profile, and in terms of OEWF is defined as

$$n_-(\eta)=3\int_0^1 dt(1-t^2)\,|\,\psi_t(\eta)\,|^2\ . \tag{6}$$

The solutions for $\psi_t(\eta)$ in Eq. (5) can be written as

$$\psi_t(\eta)=y^\mu u(y)\ , \tag{7}$$

where

$$y=-\exp[(\eta-\eta_0)/\alpha]\ .$$

Now, setting $\mu=\alpha(\lambda^2-t^2)^{1/2}$, Eq. (5) can be recast into a hypergeometric equation of the form

$$y(1-y)u''+(1-y)(1+2\mu)u'-\lambda^2\alpha^2u=0\ , \tag{8}$$

where u' and u'' are the first and the second derivatives of u with respect to η, respectively. Here the boundary condition is such that $u(y=0)=$constant. From Eq. (8) we obtain u as

$$u={}_2F_1(\mu+i\mu_0,\mu-i\mu_0,1+2\mu,y)\ , \tag{9}$$

where $\mu_0=\alpha t$. u goes to unity for $y=0$, as required by the boundary condition, and F converges absolutely throughout the entire unit circle in the complex y plane.

Thus the bound-state solutions which enter in all quantities of our interest here are obtained as

$$\psi_t(\eta)=\frac{e^{(\eta-\eta_0)\mu/\alpha}}{2c}\times{}_2F_1(\mu+i\mu_0,\mu-i\mu_0,1+2\mu,-e^{(\eta-\eta_0)/\alpha})\ , \tag{10}$$

where c is the normalization constant.

One can make use of various transformation formulas for hypergeometric functions[10] and then by writing in series form, $\psi_t(\eta)$ can be written both for $\eta>\eta_0$ and $\eta<\eta_0$ as

$$\psi_t(\eta)=\frac{e^{(\mu/\alpha)(\eta-\eta_0)}}{2c}\left[1+\sum_{k=1}^{\infty}b_k e^{(k/\alpha)(\eta-\eta_0)}\right]\quad\text{for }\eta<\eta_0 \tag{11}$$

and

$$\psi_t(\eta)=-\operatorname{Im}\left[e^{-i[\delta(t)+(\eta-\eta_0)t]}\left[1+\sum_{k=1}^{\infty}a_k e^{-(k/\alpha)(\eta-\eta_0)}\right]\right]\quad\text{for }\eta>\eta_0\ , \tag{12}$$

where

$$\left[\frac{1}{2c}\right]^2=\frac{t^2}{\lambda^2}\prod_{k=1}^{\infty}\left[1+\frac{4\alpha^2t^2}{k^2}\right]\left[1+\frac{\alpha^2\lambda^2}{k(k+2\mu/\alpha)}\right]^{-2}\ , \tag{13a}$$

$$b_k=\frac{(-1)^k}{k!}\frac{\Gamma(k+\mu+i\mu_0)\Gamma(k+\mu-i\mu_0)\Gamma(1+2\mu)}{\Gamma(k+1+2\mu)\Gamma(\mu+i\mu_0)\Gamma(\mu-i\mu_0)}\ , \tag{13b}$$

and

$$a_k=\frac{(-1)^k}{k!}\frac{\Gamma(k+\mu+i\mu_0)\Gamma(k-\mu+i\mu_0)\Gamma(1-2\mu)}{\Gamma(k+1-2\mu)\Gamma(\mu+i\mu_0)\Gamma(-\mu+i\mu_0)} . \tag{13c}$$

Here $\delta(t)$ is the phase shift defined as

$$\delta(t)=\tan^{-1}\left[\frac{\mu_0}{\mu}\right] - \sum_{n=1}^{\infty}\left[2\tan^{-1}\left[\frac{\mu_0}{\mu+n}\right]-\tan^{-1}\left[\frac{2\mu_0}{n}\right]\right], \tag{14}$$

such that as $\eta\to\infty$, $\psi_t(\eta)$ tends to the form [to be consistent with the definition of $n_-(\eta)$ in Eq. (6)]

$$\psi_t(\eta)\to\sin[t(\eta-\eta_0)+\delta(t)] \text{ as } \eta\to\infty . \tag{15}$$

It can be seen that for $\alpha=0$, $\delta(t)$ reduces to $\tan^{-1}[t(\lambda^2-t^2)^{-1/2}]$, which is the phase-shift factor obtained in the FB model. An expression for η_0, the metal position parameter, is obtained from the overall charge-neutrality requirement, i.e.,

$$\int_{-\infty}^{\infty} n_T(\eta)d\eta=0 , \tag{16}$$

where $n_T(\eta)=n_-(\eta)-\Theta(\eta)$ and $\Theta(\eta)$ is the usual step function

$$\eta_0=\int_{-\infty}^{\eta_0} n_-(\eta)d\eta+\int_{\eta_0}^{\infty}[n_-(\eta)-1]d\eta . \tag{17}$$

The electrostatic potential $v_{es}(\eta)$ is obtained in the present choice of origin of the axes as a solution of Poisson's equation:

$$\frac{d^2}{d\eta^2}v_{es}=-\frac{8}{3\pi k_F}n_T(\eta) . \tag{18}$$

Applying the charge-neutrality condition, together with the boundary conditions $v_{es}(\infty)=0$ and $v'_{es}(-\infty)=0$, the solution for v_{es} is obtained as

$$v_{es}(\eta)=-\frac{8}{3\pi k_F}\int_{-\infty}^{\eta} n_T(n')(\eta'-\eta)d\eta' , \tag{19}$$

and the surface dipole barrier contribution to the work function $\Delta\phi$ is given by the expression

$$\Delta\phi=-\frac{8}{3\pi k_F}\int_{-\infty}^{\infty} n_T(\eta')(\eta'-\eta_0)d\eta' . \tag{20}$$

We need the jump $J(\alpha,\lambda)$ in the potential as η varies from $-\infty$ to $+\infty$ [i.e., $v(-\infty)-v(\infty)$] which is reconstructed within LDA using the density profile in Eq. (6). The expression for the effective potential has the form

$$v(\eta)=-\frac{8}{3\pi k_F}\int_{\eta}^{\infty} n_T(\eta')(\eta'-\eta)d\eta' - \frac{2}{k_F^2}\mu_{xc}(\eta\to\infty)+\frac{2}{k_F^2}\mu_{xc}(n_-(\eta)) , \tag{21}$$

where μ_{xc} is the exchange and correlation part of the chemical potential. The jump now can be obtained as [making use of Eq. (16)]

$$J(\alpha,\lambda)=-\frac{8}{3\pi k_F}\int_{-\infty}^{\infty} n_T(\eta')(\eta'-\eta_0)d\eta' - \frac{2}{k_F^2}\mu_{xc}(\eta\to\infty) =\Delta\phi-\frac{2}{k_F^2}\mu_{xc}(\eta\to\infty) , \tag{22}$$

where $\Delta\phi$ is given by the expression in Eq. (20). Now, as a self-consistent requirement this should be the same as $\lambda^2(=V_0/\epsilon_F)$, i.e.,

$$J(\alpha,\lambda)=\lambda^2 . \tag{23}$$

Lastly, we impose another physical constraint which relates the difference in electrostatic potential between that at the surface and deep inside the metal to the bulk properties. According to the theorem due to Budd and Vannimenus,[7] this difference is related to the energy per electron for the uniform electron gas:

$$\Delta v_{es}=v_{es}(\eta=0)-v_{es}(\eta\to\infty) =0.4-0.0829r_s-\frac{0.0796r_s^3}{(r_s+7.8)^2} , \tag{24}$$

where r_s is the electron density parameter, $r_s^3=3/4\pi\bar{n}$, and $\bar{n}$ is defined by $3\pi^2\bar{n}=k_F^3$. In the present case, this difference is equal to

$$\Delta v_{es}=-\frac{8}{3\pi k_F}\int_0^{\infty}[n_-(\eta)-\Theta(\eta)]\eta\,d\eta . \tag{25}$$

The right-hand side of Eq. (24) depends only on r_s which is a bulk parameter. Thus, by this simple theorem, the difference in the electrostatic potential from its surface to inside value is related to r_s.

In all these expressions [Eqs. (17), (22), and (25)] it is possible to evaluate the spatial integrals analytically using the expression in Eq. (5) for the charge density. Finally, the expressions we obtain for computation are in the form of infinite series with a few integrals (integral over $t=k/k_F$) to be evaluated numerically. These equations are solved iteratively for λ and α using the Newton-Raphson numerical solution method, with the Gaussian quadrature method for evaluating the integrals. The software developed for this program are quite general for the use of the Newton-Raphson method for two variables and a separate subroutine for Gaussian quadrature is used. This is well optimized and usually takes about a minute on a Digital PDP-10 system.

The various expressions for η_0, $\Delta\phi$, and Δv_{es} in terms of λ and α are as follows:

(a) Expression for η_0:

$$\eta_0=-\frac{3\pi}{8}+3\int_0^1 dt(1-t^2)\left[\alpha(I_1-I_2)+\frac{\sin[2\delta(t)]}{4t}\right], \tag{26}$$

where

$$I_1=\left[\frac{1}{2c}\right]^2\left[\frac{1}{2\mu}+2\sum_{k=1}^{\infty}\frac{b_k}{k+2\mu}+\sum_{k,k'=1}^{\infty}\frac{b_k b_{k'}}{k+k'+2\mu}\right]$$

and

$$I_2=\mathrm{Re}\left[\sum_{k=1}^{\infty}\left[\frac{a_k e^{-2i\delta}}{k+2i\mu_0}-\frac{a_k}{k}\right]+\tfrac{1}{2}\sum_{k,k'=1}^{\infty}\left[\frac{a_k a_{k'} e^{-2i\delta}}{k+k'+2i\mu_0}-\frac{a_k a_{k'}^*}{(k+k')}\right]\right].$$

(b) Expression for $\Delta\phi$ (in units of ϵ_F):

$$\left[\frac{-3\pi k_F}{8}\right]\Delta\phi=\frac{\eta_0^2}{2}+\frac{3\pi}{8}\delta'(t=0)-3\int_0^1 dt(1-t^2)\alpha^2\left[S_1+S_2+\frac{1}{(2\mu)^2}\right]-\tfrac{3}{4}\int_0^1 dt\left[\cos(2\delta)+(1-t^2)\frac{\sin(2\delta)}{t}\delta'(t)\right], \tag{27}$$

where

$$S_1=\sum_{k=1}^{\infty}\left[\frac{2b_k}{(2c)^2(k+2\mu)^2}+\mathrm{Re}\left[\frac{a_k e^{-2i\delta}}{(k+2i\mu_0)^2}-\frac{a_k}{k^2}\right]\right]$$

and

$$S_2=\sum_{k,k'=1}^{\infty}\left[\frac{b_k b_{k'}}{(2c)^2(k+k'+2\mu)^2}+\mathrm{Re}\left[\frac{a_k a_{k'} e^{-2i\delta}}{2(k+k'+2i\mu_0)^2}-\frac{a_k a_{k'}^*}{2(k+k')^2}\right]\right].$$

(c) Expression for Δv_{es} (in units of ϵ_F):

$$\left[\frac{3\pi k_F}{8}\right]\Delta v_{\mathrm{es}}=-\frac{3\pi}{8}[\delta'(t=0)-\eta_0]+3\alpha^2\int_0^1 dt(1-t^2)\mathrm{Re}S_3$$
$$+\tfrac{3}{4}\int_0^1 dt\{\cos[2(\eta_0 t-\delta)]-(1-t^2)\sin[2(\eta_0 t-\delta)][\delta'(t)-\eta_0]\}, \tag{28}$$

where

$$S_3=\sum_{k=1}^{\infty}a_k e^{(k/\alpha)\eta_0}\left[\frac{e^{-2i(\delta+\eta_0 t)}}{(k+2i\mu_0)^2}-\frac{1}{k^2}\right]+\tfrac{1}{2}\sum_{k,k'=1}^{\infty}e^{[(k+k')/\alpha]\eta_0}\left[\frac{e^{-2i(\delta+\eta_0 t)}a_k a_{k'}}{(k+k'+2i\mu_0)^2}-\frac{a_k a_{k'}^*}{(k'+k)^2}\right].$$

In all these expressions, it is easy to see that as $\alpha\to 0$, these tend to the expressions obtained in the FB model.

The work function for a semi-infinite jellium Φ^J is simply obtained as (in units of ϵ_F)

$$\Phi^J(\epsilon_F)=\lambda^2-1. \tag{29}$$

For the real metal case, wherein the ion-lattice effects are introduced via the local pseudopotentials, the expression for the work function reduces to[9]

$$\Phi(\epsilon_F)=\lambda'^2-1-\langle\delta v\rangle_{\mathrm{av}}, \tag{30}$$

where $\langle\delta v\rangle_{\mathrm{av}}$ is the average value of $\delta v(r)$ over the volume of the semi-infinite crystal. Here λ' (different from λ in value) is determined iteratively from the jump in the potential with the inclusion of lattice effects. As the density profile changes slightly on introduction of ion-lattice effects, the results for surface dipole barrier show a change. These in turn are reflected in the change of values in λ and Φ. For the densely packed crystal faces $\langle\delta v\rangle_{\mathrm{av}}$ is obtained as[9]

$$\langle\delta v\rangle_{\mathrm{av}}=\frac{k_F^3}{3\pi}\left[2r_c^2-\frac{d^2}{6}\right], \tag{31}$$

for the choice of Ashcroft pseudopotential[11] $\omega(r)$ of the form

$$\omega(r)=-\frac{z}{r}[1-\Theta(r_c-r)]. \tag{32}$$

Here z is the ionic charge and r_c is a cutoff radius. The choice of r_c for each metal is such that it gives a good description of the bulk properties. d in Eq. (31) represents the interplanar spacing.

TABLE I. Results of work-function $\Phi^J(\epsilon_F)$ values and the potential parameter, viz., the barrier height parameter λ, the metal position parameter η_0, and the exponential parameter α, for the one-electron potential model of Woods-Saxon type are shown in the jellium-model approximation. $\Phi^J(\epsilon_F)$ values of (a) fully self-consistent calculations of Lang and Kohn (LK), (b) finite-barrier model-potential calculations (FB), and (c) finite-linear potential-model calculations (FL) are quoted. r_s is the Wigner-Seitz radius.

				$\Phi^J(\epsilon_F)$			
r_s	λ	$-\eta_0$	α	Present	LK[a]	FB[b]	FL[c]
2.0	1.096	0.462	0.514	0.201	0.31	0.053	0.334
2.5	1.173	0.521	0.431	0.376	0.464	0.342	0.463
3.0	1.245	0.532	0.343	0.550	0.628	0.639	0.600
3.5	1.313	0.501	0.242	0.724	0.797	0.807	0.743
4.0	1.379	0.407	0.035	0.902	0.978	0.891	0.891

[a]See Ref. 1
[b]See Ref. 4.
[c]See Ref. 5.

III. RESULTS

In Table I the values for λ, α, and η_0, obtained from our approximate self-consistent scheme as discussed in Sec. II, are presented. In the same table, the values for work function Φ^J for the jellium model obtained in the present scheme as well as those of Lang and Kohn obtained via fully self-consistent calculations and other LDA calculations[4,5] are also presented.

In Table II the work-function values for the principal faces of a few simple metals (Al, Zn, Li, Ca, Sr, Ba, and Na) obtained by using the expression in Eq. (30) for $\Phi(\epsilon_F)$ and Eq. (29) for $\Phi^J(\epsilon_F)$ are presented. A detailed comparison of these results with experimental values is not possible since the experimental values are available only for polycrystalline samples. Nevertheless, we compare our results with the available polycrystalline experimental values only, since the anisotropies among different faces are typically of the order of 10% of the mean work-function values.[1] For comparison sake we also present in the same table the results for both $\Phi(\epsilon_F)$ and $\Phi^J(\epsilon_F)$, obtained by Sahni and Gruenebaum[9] for the finite-linear potential model. They have obtained $\Phi(\epsilon_F)$ for these simple metals, with wave-vector correction to the local exchange and correlation energy functional.

As Table I indicates, our results for semi-infinite jellium compare well with those of Lang and Kohn for the range $r_s=2$ to 4. As r_s increases, the comparison improves and it is interesting to note that for about $r_s=4$, all the three model potentials, namely, FB, FL, and the present model potentials, give almost the same results. This is true since as we have mentioned earlier, as $\alpha\rightarrow 0$ our model reduces to the FB model and it can be seen that from Table I for $r_s=4$, the value of α ($=0.035$) is very small. This is also true in the FL potential-model case since it reduces to the FB model as the slope parameter tends to zero. From the FL model as well as from the present model analysis it can be drawn that for $r_s>4$, it is safe enough to use the finite-barrier potential model. However, for smaller r_s (~ 2), the FB model fails com-

TABLE II. Work-function values of real metals $\Phi(\epsilon_F)$ with local pseudopotential approximation for ion-lattice effects, as well as for the jellium model $\Phi^J(\epsilon_F)$. The results of Sahni and Gruenebaum for both $\Phi(\epsilon_F)$ as well as $\Phi^J(\epsilon_F)$, and the polycrystalline experimental values are quoted from Ref. 9. Faces shown are the most densely packed crystal faces of the metals, respectively, and $\langle \delta v \rangle_{av}$ is the average of the discrete-lattice perturbation over the volume of the semi-infinite crystal. r_s and r_c are the Wigner-Seitz and pseudopotential core radii, respectively.

					$\Phi^J(\epsilon_F)$		$\Phi(\epsilon_F)$		
Metal	Face	r_s	r_c	$\langle \delta v \rangle_{av}(\epsilon_F)$	Present	Sahni-Gruenebaum[a]	Present	Sahni-Gruenebaum[a]	Experiment[a]
Al(fcc)	(111)	2.07	1.12	−0.145	0.226	0.287	0.255	0.297	0.358
Zn(hcp)	(0001)	2.30	1.27	−0.073	0.304	0.371	0.314	0.385	0.457
Li(bcc)	(110)	3.28	1.06	−0.180	0.649	0.749	0.661	0.831	0.665 (0.498)
Ca(fcc)	(111)	3.28	1.73	−0.026	0.649	0.749	0.649	0.790	0.616
Sr(fcc)	(111)	3.57	1.93	0.013	0.748	0.875	0.747	0.908	0.659
Ba(bcc)	(110)	3.69	2.01	0.071	0.788	0.927	0.786	0.976	0.734
Na(bcc)	(110)	3.99	1.67	0.001	0.888	1.054	0.889	1.057	0.857

[a]See Ref. 9.

pletely whereas the other two models give better results. We have an advantage over the FL model in that ours does not require much mathematical labor and is computationally a simple one. In the FL potential-model calculations, the OEWF are obtained in terms of the Airy functions and their first derivatives (see Ref. 5) whereas in the present case, these are obtained in simple infinite series form that converges sufficiently fast. This makes the use of OEWF obtained in the present scheme for the further study, viz., in linear response theory, simpler compared to the FL potential-model calculations.

From Table II it can be seen that our results for simple metals are tallying well with the polycrystalline experimental values. For the simple metals we considered here, the difference between $\Phi(\epsilon_F)$ and $\Phi^J(\epsilon_F)$ is very small (within $<10\%$ of each other) owing to the fact that $\langle \delta v \rangle_{\rm av}$ is finite and cancels the effect of change in the relaxation dipole barrier on inclusion of the ionic pseudopotential. Our Φ^J results for the jellium model show an improvement over the results of Sahni and Gruenebaum[9] for larger r_s values in comparison with polycrystalline experimental values. The work-function values Φ^J for the simple metals Li, Ca, Sr, Ba, and Na are within 10% of the polycrystalline experimental values. However, for Al and Zn, they are about 20% different from their respective experimental values.

In conclusion we note that the present analysis with a Woods-Saxon type of potential model does lead to consistent results, and the OEWF thus obtained are simple enough to enable us to use them for further studies.

[1]N. D. Lang and W. Kohn, Phys. Rev. B **1**, 4555 (1970); **3**, 1215 (1971).

[2]W. Kohn and L. J. Sham, Phys. Rev. **140**, A1133 (1965); N. D. Lang, in *Solid State Physics, Advances in Research and Applications,* edited by H. Ehrenreich, F. Seitz, and D. Turnbull (Academic, New York, 1973), Vol. 28, p. 243.

[3]P. J. Feibelman, Phys. Rev. B **12**, 1319 (1975); **22**, 3654 (1980).

[4]V. Sahni, J. B. Krieger, and J. Gruenebaum, Phys. Rev. B **12**, 3505 (1975); P. Raghavendra Rao and G. Mukhopadhyay, Nucl. Phys. Solid State Phys. (India) **24C**, 1 (1981).

[5]V. Sahni, J. B. Krieger, and J. Gruenebaum, Phys. Rev. B **15**, 1941 (1977); V. Sahni, C. Q. Ma, and J. S. Flamholz, *ibid.* **18**, 3931 (1978).

[6]P. Raghavendra Rao and G. Mukhopadhyay, Nucl. Phys. Solid State Phys. (India) (to be published).

[7]H. F. Budd and J. Vannimenus, Phys. Rev. Lett. **31**, 1218 (1973); **31**, 1430(E) (1973); J. Vannimenus and H. F. Budd, Solid State Commun. **15**, 1739 (1974).

[8]P. Raghavendra Rao and G. Mukhopadhay, Solid State Commun. (to be published).

[9]V. Sahni and J. Gruenebaum, Phys. Rev. B **19**, 1840 (1979).

[10]I. S. Gradshteyn and I. M. Ryzhik, *Tables of Integrals, Series and Products* (Academic, New York, 1965), p. 1043.

[11]N. W. Ashcroft, Phys. Lett. **23**, 48 (1966).